MASTER

UCID- 17585

Lawrence Livermore Laboratory

BUILDING 431 FIRE TESTS

N. J. Alvares
D. G. Beason
H. W. Ford
M. W. Magee

October 24, 1977

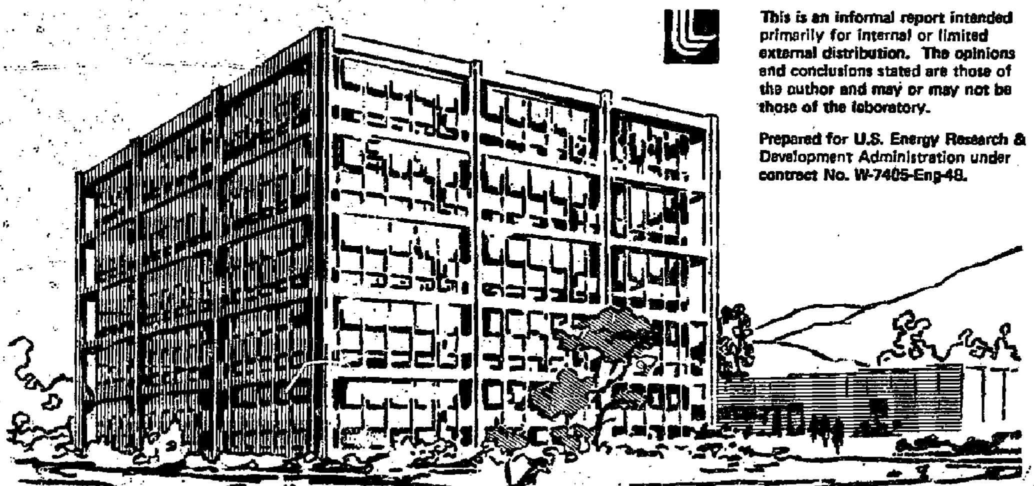

This is an informal report intended primarily for internal or limited external distribution. The opinions and conclusions stated are those of the author and may or may not be those of the laboratory.

Prepared for U.S. Energy Research & Development Administration under contract No. W-7405-Eng-48.

BUILDING 431 FIRE TESTS

INTRODUCTION

Building 431 is being remodeled to accept the Mirror Fusion Test Facility (MFTF). Within the remodeling schedule was a period of time when there would be no activity in the shielded area which had been occupied by the Astron Accelerator. A similar shielded area will be required for the MFTF device. This enclosure will contain a complex mix of electrical and thermal insulators, power and diagnostic equipment, and a large volume of dielectric fluid, all of which have some flammable potential. Because of this potential, adequate fire protection must be provided within the shielding. The fire management system designed for this facility must have the capability of early warning detection of incipient fires, and the capacity to suppress any fire that could compromise the progress of the experiment.

The current state-of-the-art of fire protection is quite adequate for common structures, but very little guidance is available for the design of fire management systems to protect massive high-energy equipment in huge high-bay enclosures. Similarly, abundant fire dynamics data are available for bedroom-size enclosures, and some smoke movement studies have been conducted in commercial buildings. The only fire studies which have been conducted in large enclosures show that fires behave in a manner that is unique to the enclosure. Therefore, it is virtually impossible to use the findings of such tests to predict the fire dynamics and smoke movement characteristics in uniquely different enclosures, particularly when the fuel components are not similar.

Because of this situation, the Fire Safety Group at LLL proposed to the Fire Research Steering Committee that Special Projects Division conduct fire tests in the Astron bay of Bldg. 431. The specific areas of concern that prompted the proposal are:

- How does the bouyant smoke plume interact with the normal ventilation patterns of the building?
- Does Building 431 have a resident inversion layer? (i.e., in hot weather does a layer of hot air form near the ceiling that would prevent penetration of fire-generated heat and smoke to the ceiling?)

- How long does it take for smoke to reach the ceiling? To fill the ceiling space? To fill the shielded area? To activate strategically placed detection arrays?
- What is the temperature rise in the high bay ceiling? In the shielded area? At the detector arrays for various fire sizes and types?
- Will existing ceiling vents remove significant quantities of smoke and heat?
- Under venting conditions, will the ceiling air temperature rise be of sufficient rate to potentially fuse the ceiling sprinklers? (i.e., will the sprinklers fuse before the fire grows to a size that is difficult to control?)
- What type(s) of detector responds most reliably to the types and sizes of fires that have some probability of occurrence in the MFTF arena?
- What types of fire suppression strategies provide a feasible solution to the major potential fuel sources projected for the enclosure?
- What logic can be used to identify sites for location of detection and suppression arrays?
- Which components of smoke are most readily detectable in large-volume enclosures?

THE EXPERIMENTAL DESIGN

The Source

Since the tests were to be conducted within an unoccupied region of a much larger and occupied building, it was desirable to have a fire source that was scalable, reproducible, easily controlled, and would produce a combustion product aerosol with characteristics similar to those produced by insulation polymers and dielectric fluids. However, because of the other residents of the building, we were constrained to use a fuel which was not too smokey. Review of the literature of fuels indicated that n-heptane (C_7H_{16}) possessed the desirable characteristics. Consequently, fully turbulent pool fires [pool diameters greater than 0.9 m (3.0 ft)] were proposed for the majority of the test fires. The selected diameters were 0.9 m (3 ft), 1.8 m (6 ft), and 3 m (10 ft), respectively. The 0.9- and 1.8-m pools were contained in existing circular steel pans designed specifically for pool fire tests. The pans were half-filled with water and a layer of fuel was floated on top of the water.

After conducting several fires of these two sizes, we found it unnecessary to conduct the 3-m fires.

It was also desirable to conduct some fires using cellulosic materials. We chose to bunch computer paper in a 0.9 × 1.2 m (3 × 4 ft) cage to simulate the type of fire that might occur in waste paper areas near diagnostic computer arrays.

Both the cellulosic cage fires* and the 0.9-m pan fires were placed on an automatic weight-measuring platform (load cell). The load-cell measurements allowed us to determine the fuel consumption rate for the smaller test fires. Figures 1 and 2 show the test pans and the cellulosic cage, respectively.

The specific site for the fire tests was the center of the accelerator "bunching ring," [i.d. = 6.6 m (22 ft)]. Simple geometric calculations indicated that the maximum thermal radiation from the flame plume to the inside surface of the ring would be 1.2 W/cm^2. We anticipated little damage from this irradiance level; however, to ensure safety we lined the inside perimeter of the ring with gypsum board. Figure 3 shows the fire site set up for 0.9-m pan burns.

Diagnostic Instrumentation

Figure 4 is a sketch of the burn site location from top and side view. (Note that the sketch is not to scale and the station and instrument locations are approximate.)

Diagnostic instrumentation included thermocouples for temperature measurements, radiometers to sense the magnitude of the thermal radiation and total heat convective field at specific locations, photographic and television monitoring for fire dynamics and smoke flow studies, and measurement of the mass loss rate of fuel with a load cell to determine the combustion heat release rate.

Thermocouples and radiometers were located at all three instrumentation stations shown in the sketch. In addition, a string of variably spaced thermocouples was suspended from the ceiling of the building to just over the shielding block. [There was a large opening approximately 4.5 × 10.5 m (15 × 35 ft) in the roof ceiling block where the thermocouple leads penetrate the shielded area, and from which smoke is transmitted to the main structure.] One radiometer was located 1.5 m (5 ft) off the fuel plane on the south side of the sheetrock thermal shield. Video and photographic recordings were made for each test

*Hereafter condensed to "paper cage."

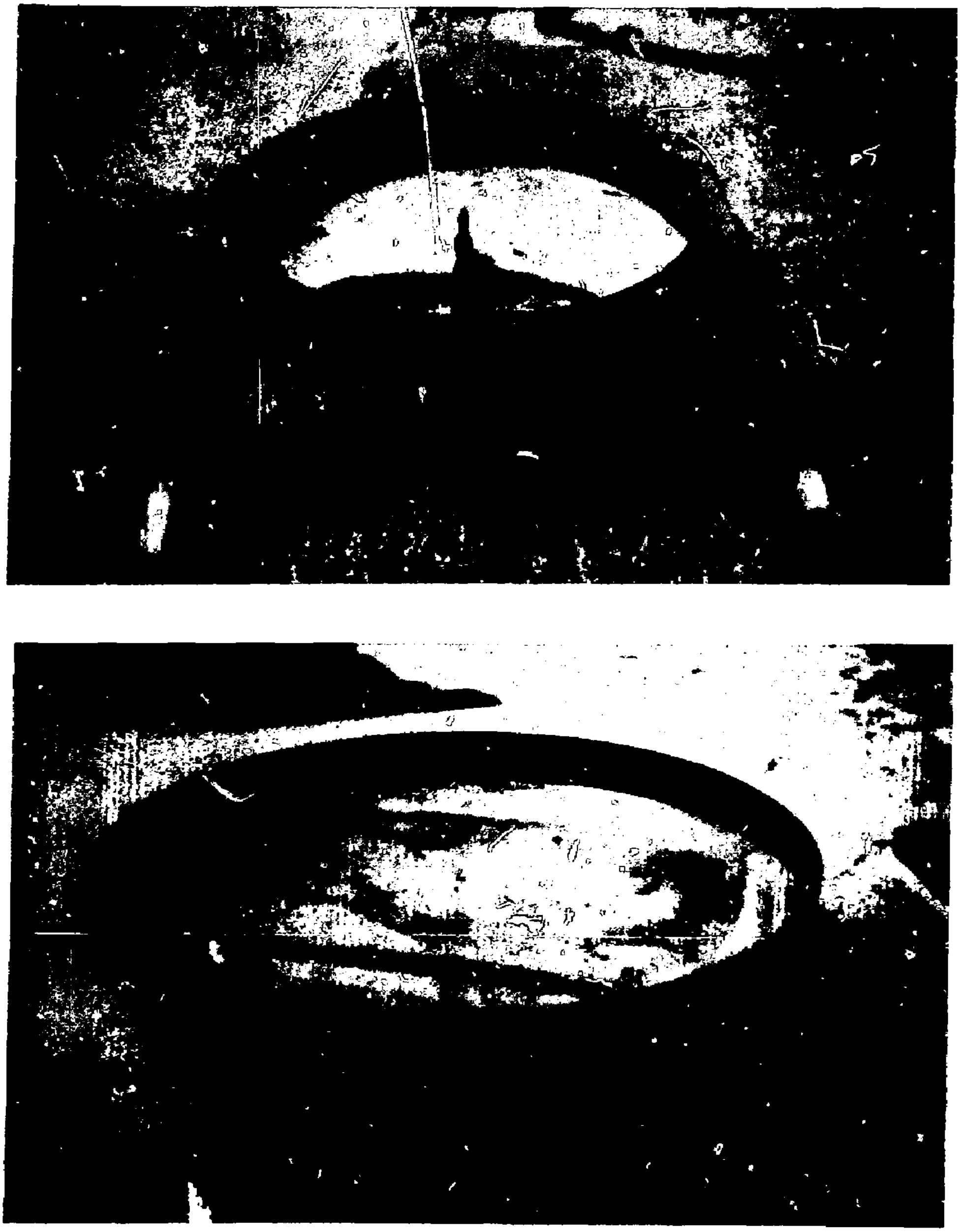

Fig. 1. Test pans. (a) 0.9-m pan and load cell; (b) 1.8-m pan.

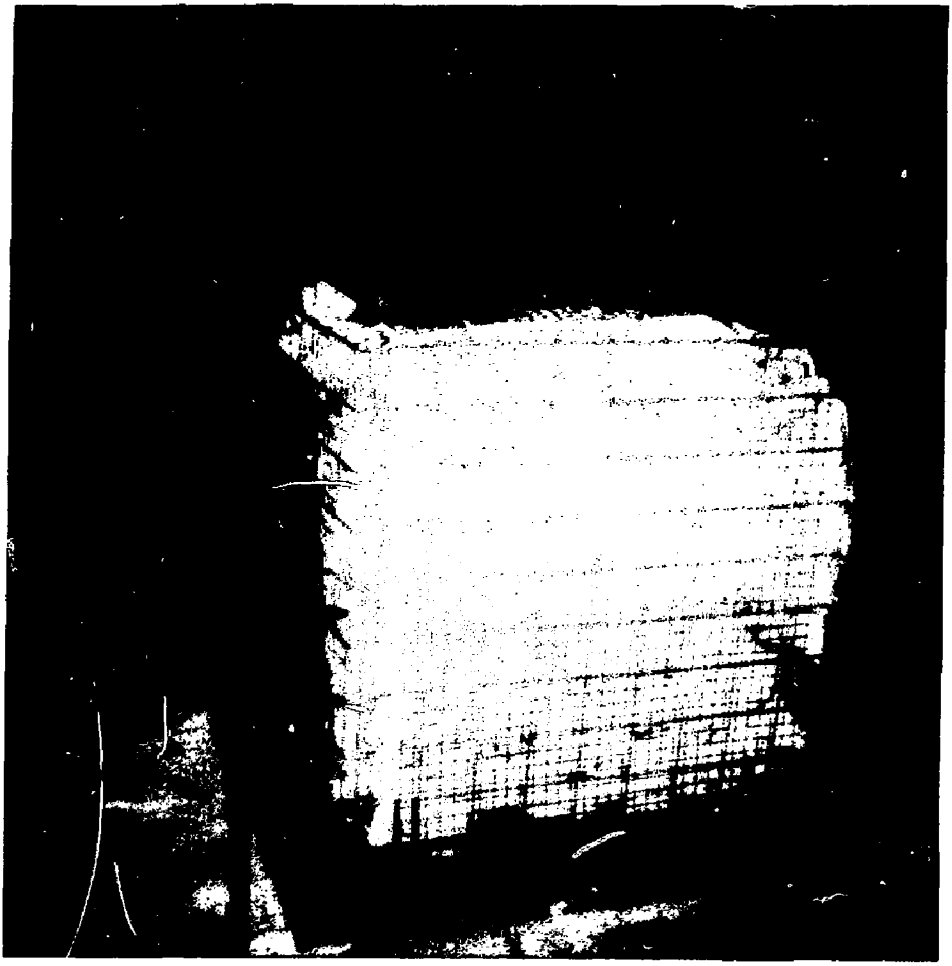

Fig. 2. Cellulosic cage test setup; 13 kg of computer paper.

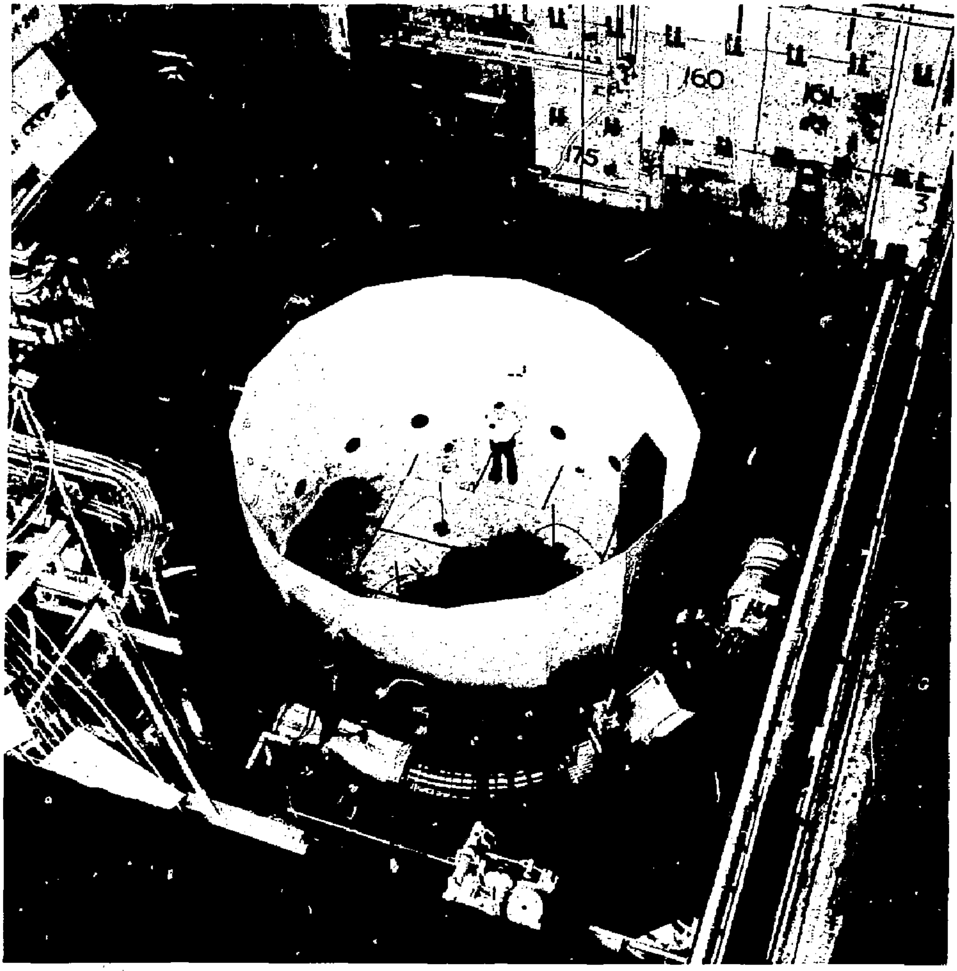

Fig. 3. Thermally shielded fire area for Bldg. 431 fire tests.

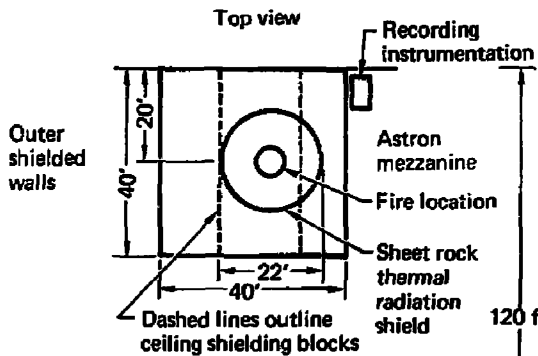

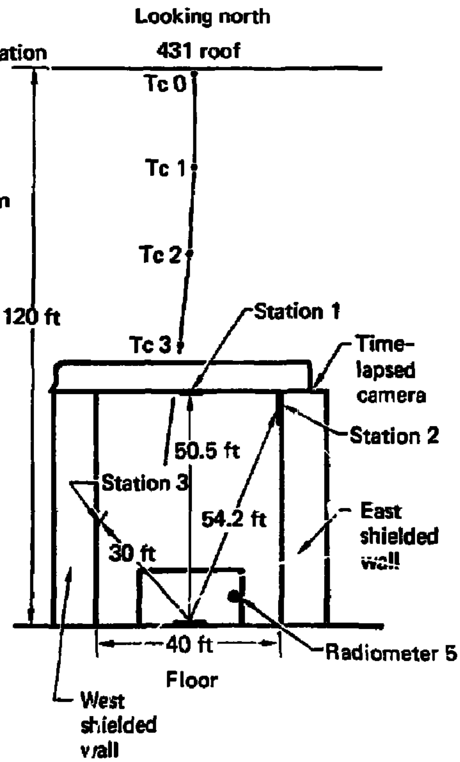

Instrumentation

Station 1	Station 2	Station 3	Fuel plane
Photoelec. (2)	Photoelec.	Photoelec.	Load cell
I.R.	I.R.	I.R.	Rad (total)
Ion (2)	Ion (2)	Ion (2)	
Thermal	Thermal	Rad (total)	
Taguchi	Rad (total)	Tc 6	
Rad (total)	Tc 5		
Rad (purge)			
Tc 4			

Fig. 4. Schematic of fire test area and instrumentation locations.

to monitor the smoke accumulation rate in the main structure and the shielded volume. Time-lapse photographic records of each fire were also taken.

The array of instrumentation listed above was adequate to define major fire and smoke characteristics for the test series. It would have been desirable to measure air velocity profiles as well to correlate with the temperature measurements. Unfortunately, lack of time and appropriate air velocity instrumentation made such measurements impossible at that time.

All diagnostic data were recorded on a Fluke 30-channel digital data logger.

Fire Detection Instrumentation

Seven types of detectors were selected for testing. They were:

Thermal detectors - Sense rate of temperature rise from combustion gases and thermal radiation from fires; essentially a bimetallic strip.

IR detectors - Sense infrared radiation from fires in a selected frequency range. Can be electronically filtered to accept radiation in the flicker frequency range of flames.

Ionization detectors - Alarms when components of flame gases intercept and reduce ion mobility current in an ion chamber field relative to a sealed cell. Rate of current decreases key's alarm.

Taguchi gas detector - A semiconductor-type device, where the absorbing surface acts as a "p" junction during normal oxygen concentrations, and an "n" junction when combustion gases are absorbed on the surface.

Photoelectric detector - Senses either the forward or side scattered light from smoke admitted into an optical cell. The intensity and/or duration of the scattered light determines the alarm.

Wilson cloud chamber - Smoke and/or combustion gases are drawn into a centrally located monitor and injected into a saturated water vapor cell. Smoke particulates act as condensation nuclei, and light scattered off the tracks is sensed as the primary alarm signal.

Beam-type detector – Will alarm in two modes: either by smoke attenuation, or by refraction of the light beam caused by the change in the index of refraction of the combustion air plume. The source light for this unit is a GaAs LED.

An array of the first six of these generic detector types was installed along with thermoccuples and radiometers on three panels which were sited at the stations indentified in Figure 4. The beam-type detector was located so that the beam intercepted the projected centerline of the burn pan at approximately 6 m (20 ft) above the fuel surface. The alarm indications from all detectors, except for the cloud chamber type, were recorded on a multichannel stripchart recorder. The cloud chamber output was on a strip chart recorder.

The instrumentation layout for the three stations is shown schematically in Fig. 5. The schematic also includes data channel designations. Figure 6 shows stations 1 and 2 looking upward from the location of the recording station.

Extinguishing Systems

Because of the large volumes involved in fusion facilities and the extremely large electrical potential of component apparatus, it is desirable to augment water sprinkler systems with extinguishers that are less water-intensive. High expansion foam (Hi-X)) is under consideration as a candidate for this purpose for regions of the MFTF enclosure. To demonstrate the utility of Hi-X, one of the tests with a 1.8-m pan fire was extinguished with a portable Hi-X generator. Most 1.8-m pool fire tests were extinguished with a commercially available agent (AFFF)* used for combating spilled liquid fuel fires. For the 0.9 m pan fires, only enough fuel was used to allow for a 3-min burn time. Note, however, the AFFF (Aqueous Film Forming Foam) system was deployed during all fire tests that were conducted in Bldg. 431. Experience with the AFFF was valuable since it is a candidate agent for protection of the large-volume dielectric oil reservoir of the neutral beam electrostatic generators. Figure 7 is a composite photograph showing the portable Hi-X generator and the AFFF system.

---

*AFF — Aqueous Film Forming Foam; more commonly known as light water.

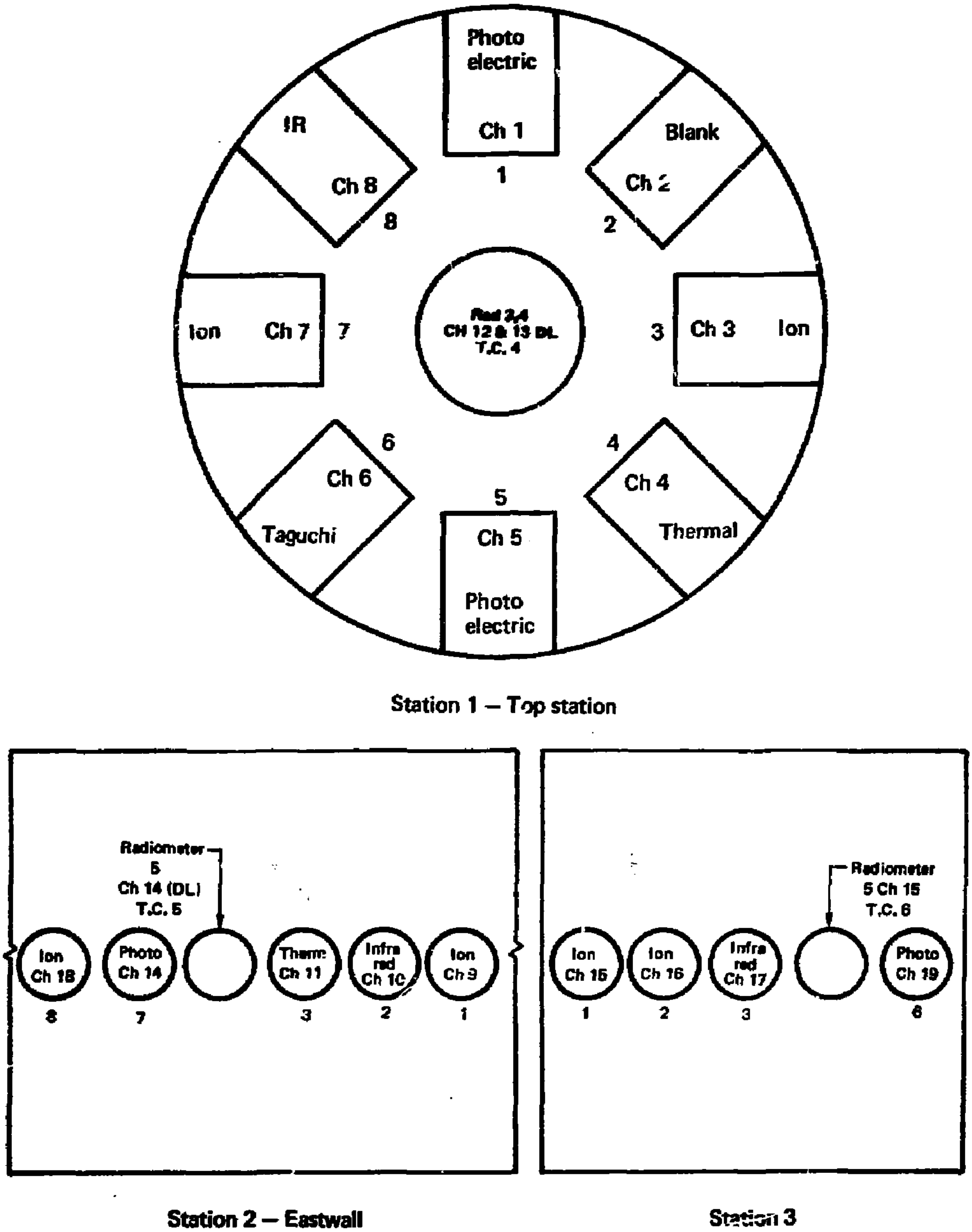

Fig. 5. Astron pit instrumentation.

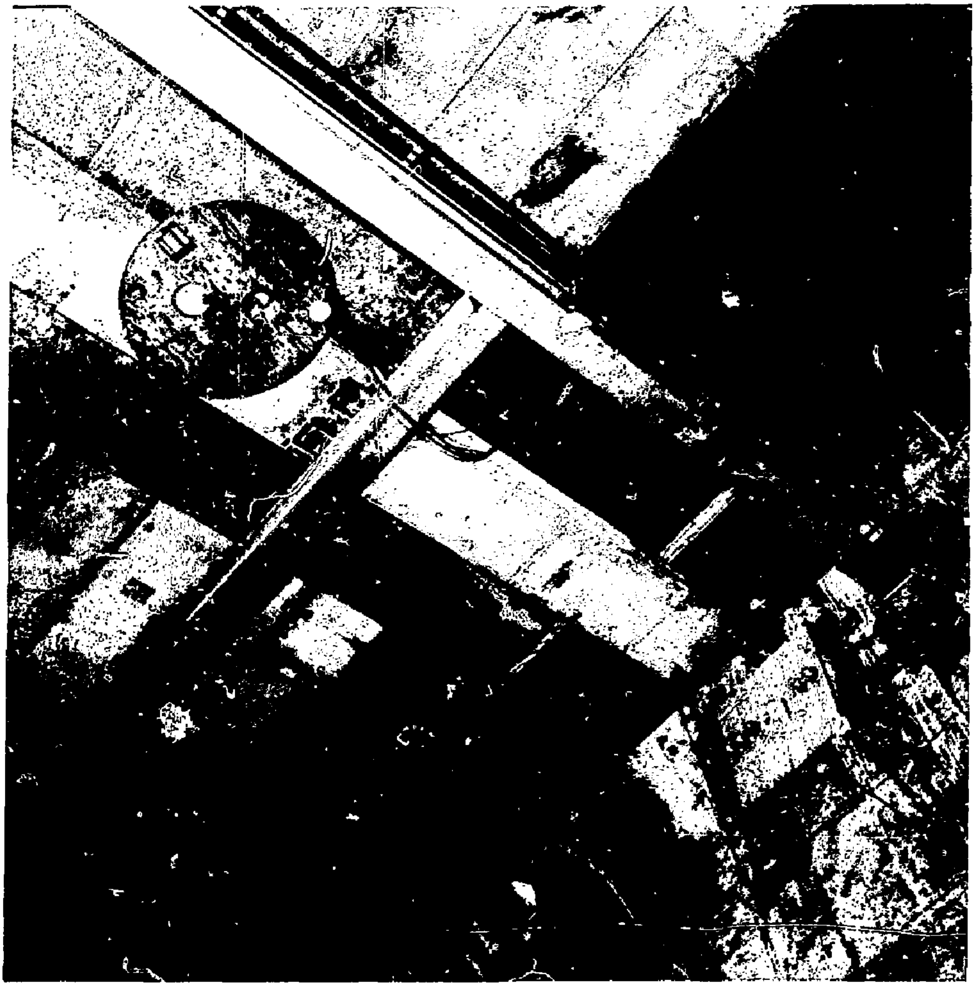

Fig. 6. Stations 1 and 2 (looking upward from recording station).

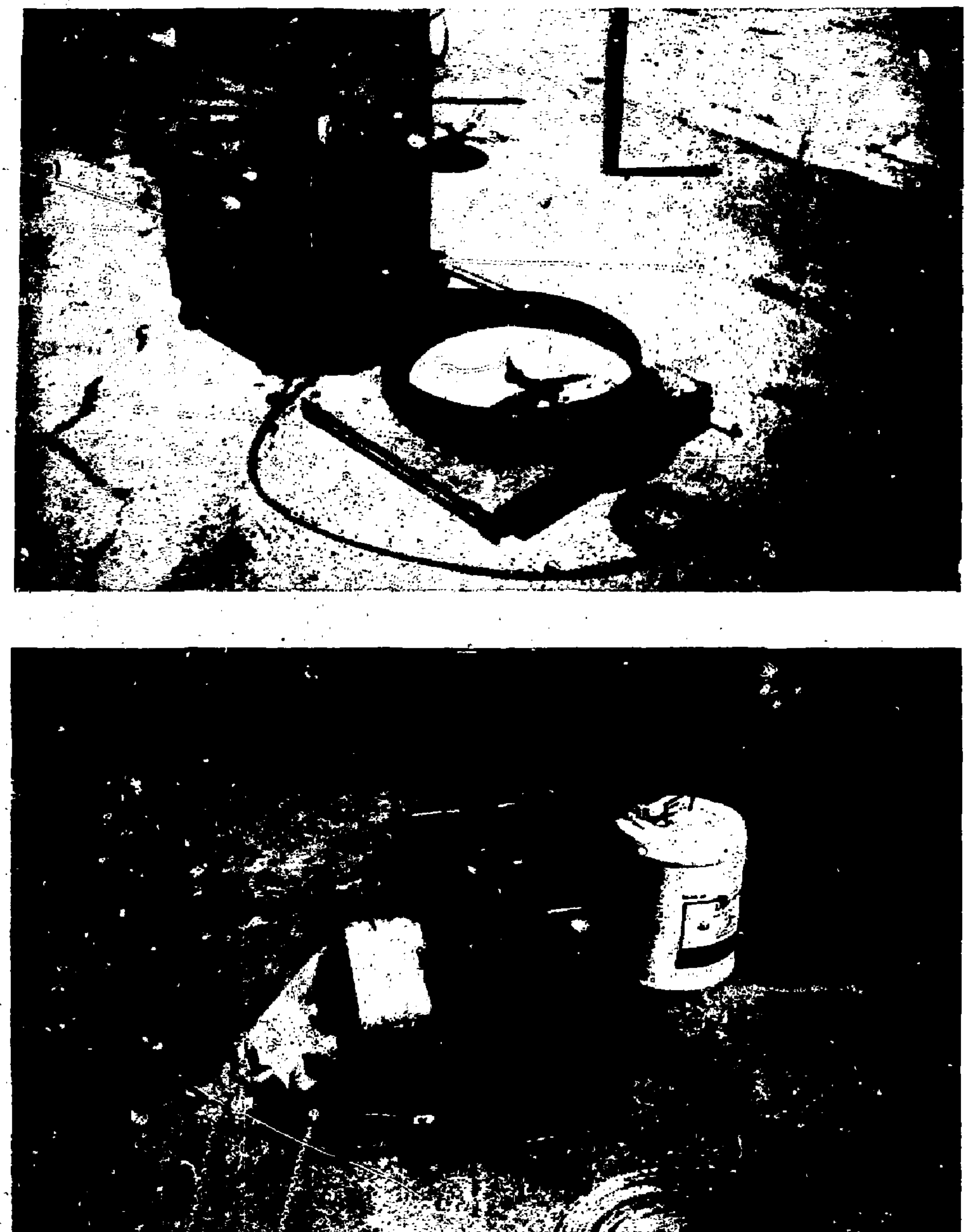

Fig. 7. (a) Portable Hi-X generator, and (b) AFFF systems.

RESULTS

Table 1 contains all the thermal data obtained during the test series, and Table 2, the detector response data. These tables essentially summarize the results of the test series.

Table 1 lists the range of temperatures in C°, and the radiation field at the positions indicated in Fig. 4. The first two columns respectively contain the pre-fire ambient temperature range for the area above and below the shielding block ceiling. Note that when a range is indicated, the first reading corresponds to the topmost thermocouple of the specific volume. The next seven columns indicate the maximum temperature rise measured during the indicated fires, as correlated by thermocouple location. The next five columns list the maximum radiant flux measured at indicated locations. The last column lists the burning rate of the fuel in kg/min of fuel consumed.

Figure 8 shows the averaged temperatures for the various tests as they vary with height above the fuel plane. The horizontal axis indicates the temperature rise, and the vertical axis indicates the thermocouple location and distance above the fuel plane. The temperature patterns for the three types of fires are similar. The minimum at position 3 probably results from the location of the thermocouple. It was over the smaller opening in the roof shielding blocks, and may have been in a flow shadow of the smoke and hot gases as they penetrated the shielding. The upper temperature pattern indicates that no inversion gradient exists in Bldg. 431 under the atmospheric conditions that existed during the tests.

The indicated temperature rise was not of sufficient magnitude to fuse sprinklers currently in residence on the Bldg. 431 ceiling. However, the fires were of relatively short duration, and the rate of temperature rise, at the ceiling, for the 1.8-m-pan fire tests is relatively fast as is indicated in Fig. 9. The rate of rise is about 0.3°C/s, but the fire duration is only 70 s. Should the fire be longer, or larger, and the ambient temperature higher (as it would be during the summer), then it is conceivable th fuse temperatures could be attained. Obviously, the smaller fires have no potential for sprinkler fusing. Note that the sharp drop in temperature at the conclusion of the 1.8-m pan fires was due to the application of an extinguishing agen. The lack of a similar drop for the 0.9-m pans is because these fires were allowe o burn out.

Table 1. Temperature and radiation summary.

Test number and type	Ambient temp (°C) (Top Δ)	Ambient temp (°C) (Bottom Δ)	Temperature rise during fire tests (°C) Channel designation 0	1	2	3	4	5	6	Thermal radiation field (Peak values)(W/cm²) 11	12	13	14	15	$\dot{m}$ (kg/min)
0.9-m pan															
1	26-21	28	4	9	15	9	17	14	9	1.1	0.1	0.15	0.14	0.15	2.8
2	29-22	29	5	7	13	11	16	15	10	2.0	0.1	0.2	0.14	0.08	2.0
3	30-23	31	4	8	15	8	15	15	8	2.0	0.1	0.16	0.14	0.15	3.0
4	18-17	20	6	8	15	7	15	14	10	1.2	0.1	0.16	0.1	0.09	2.2
		Ave.	4.75	8.0	14.5	8.75	15.75	14.5	9.25						
Paper Crib															
5	21-19	25-22	1	2	5	0	9	6	2	0.1	0.1	0.1	0.1	0.1	2.8
6	24-21	27	1	2	3	2	13	7	2	0.1	0.1	0.15	0.1	0.1	3.6
7	25-20	28	1	0	3	2	7	4	2	0.1	0.1	0.1	0.1	0.1	0.9
		Ave.	1	2	4.3	2	9.6	5.6	2						
1.8-m pan															
8	24-20	20-21	20	33	53	21	48	55	16	13.8	0	0	0	0	9.8[a]
9	28-22	30-35	21	27	51	24	47	37	15	10.7	0	1.24	0.23	0.1	9.8[a]
10	19-18	29-28	-	-	-	-	46	51	21	8.6	0	1.36	0.45	0.23	9.8[a]
		Ave.	20.5	30	52	22.5	47	47.5	17.3						

[a]Upper limit value estimated from approximate maximum heat release rate from fully turbulent hydrocarbon fuel fires.

Table 2. Detector tests – week of 11 April 1977

Fuel	Detectors alarmed	Station	Detector time	Test No. (time in seconds)				Ave.
n-heptane-0.9-m pan (2.5 gal/load)				1	2	3	4	
	8	1	IR	2.0	2.0	4.6	3.3	3.0
	7	1	Ion	13.3	14.0	18.8	17.1	15.8
	3	1	Ion	14.3	16.5	23.9	15.9	17.7
	4	1	Thermal	59.0	63.3	53.5	61.6	59.4
	1	1	Photoelectric	No	12.5	No	14.5	13.5
	10	2	IR	2.5	3.0	5.5	4.0	3.8
	13	2	Photoelectric	20.3	22.0	28.9	23.7	23.7
	9	2	Ion	45.0	No	No	No	45.0
	18	2	Ion	62.0	86.0	61.8	62.4	68.1
	11	2	Thermo	100.0	85.0	No	No	
	17	3	IR	12.0	13.5	15.2	13.0	13.4
	1	Cloud chamber		No	No	No	No	
	2	Cloud chamber		No	No	No	No	
	3	Cloud chamber		No	No	No	No	
			Beam type					
	Refractive index				19.5	39.0	37.2	31.9
	Attenuation				No	No	No	
Computer paper in-a cage				5	6	7		Ave.
	7	1	Ion	16.8	15.8	21.8		18.1
	3	1	Ion	21.8	16.0	25.7		21.2
	8	1	IR	36.7	56.3	2.7[c]		–
	1	1	Photoelectric	No	No	22.1		22.1
	10	2	IR	50.5	74.2	42.9		55.9
	17	3	IR	38.0	53.6	47.2		46.3
	1	Cloud chamber		Yes[a]	60 s[a]	60 s[a]		~60
	2	Cloud chamber		Yes	75	Yes		~75
	3	Cloud chamber		Yes	75	Yes		
			Beam type					
	Refractive index			38.7	25.7	54.1		39.5
	Attenuation			No	No	No		
Initial weight (kg)				13.kg	9	2		
n-heptane-1.8-m pan (7.0 gal/load)				8	9	10		Ave
	8	1	IR	3.5	4.5	2.3		3.4
	3	1	Ion	9.4	11.1	7.1		9.2
	7	1	Ion	10.4	9.2	7.2		8.9
	1	1	Photoelectric	11.2	No	8.9		7.8
	4	1	Therm	15.5	16.7	14.0		15.4
	5	1	Photoelectric	29.7	36.6	37.4		34.6
	6	1	Taguchi	44.6	44.7	46.3		45.2
	1	1	Cloud chamber	60.0[a]	60.0[a]	75.0[a]		65.0
	1	1	Beam type	No	No	No		
	10	2	IR	4.3	6.3	2.3		4.3
	18	2	Ion	15.9	14.9	11.3		14.0
	13	2	Photoelectric	16.7	No	13.4		15.1
	11	2	Therm	22.4	23.2	23.2		22.9
	14	2	Photo	33.2	28.4	25.2		28.9
	17	3	IR	14.1	14.7	13.3		14.0

[a] Not discriminating channels (8 and 9 at high sensitivity, 10 at low sensitivity).
[b] Indicates no alarm signal for this fire.
[c] Detector apparently caught the flash of ignition flame.

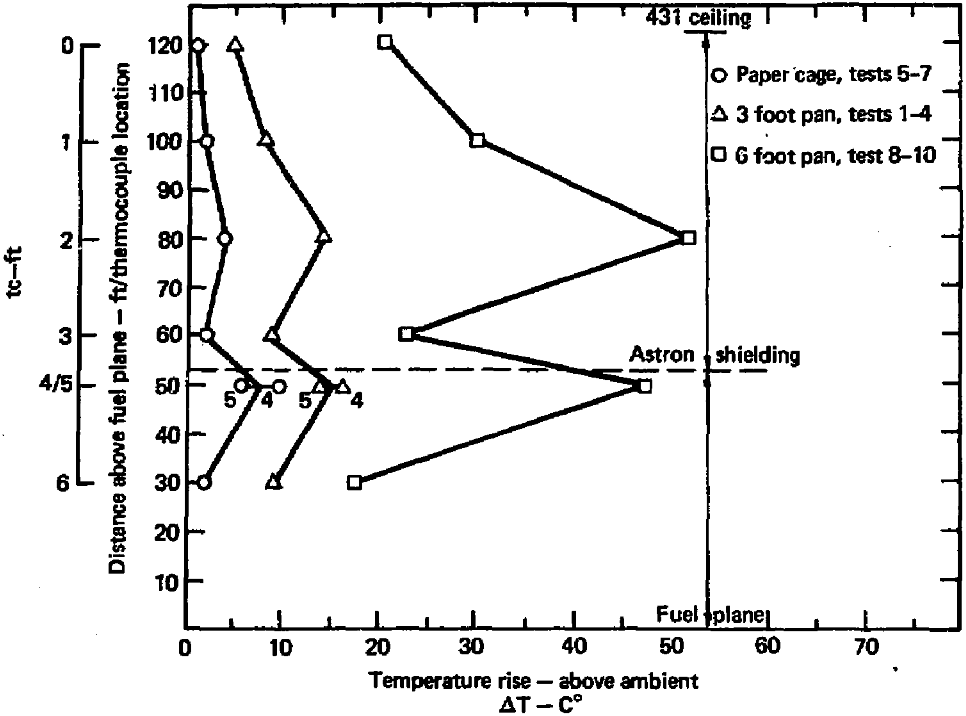

431 ceiling
Paper cage, tests 5-7
3 foot pan, tests 1-4
6 foot pan, test 8-10
Astron shielding
Fuel plane
tc—ft
0
1
2
3
4/5
6
Distance above fuel plane — ft/thermocouple location
120
110
100
90
80
70
60
50
40
30
20
10
5
4
5
4
0
10
20
30
40
50
60
70
Temperature rise — above ambient
ΔT — C°

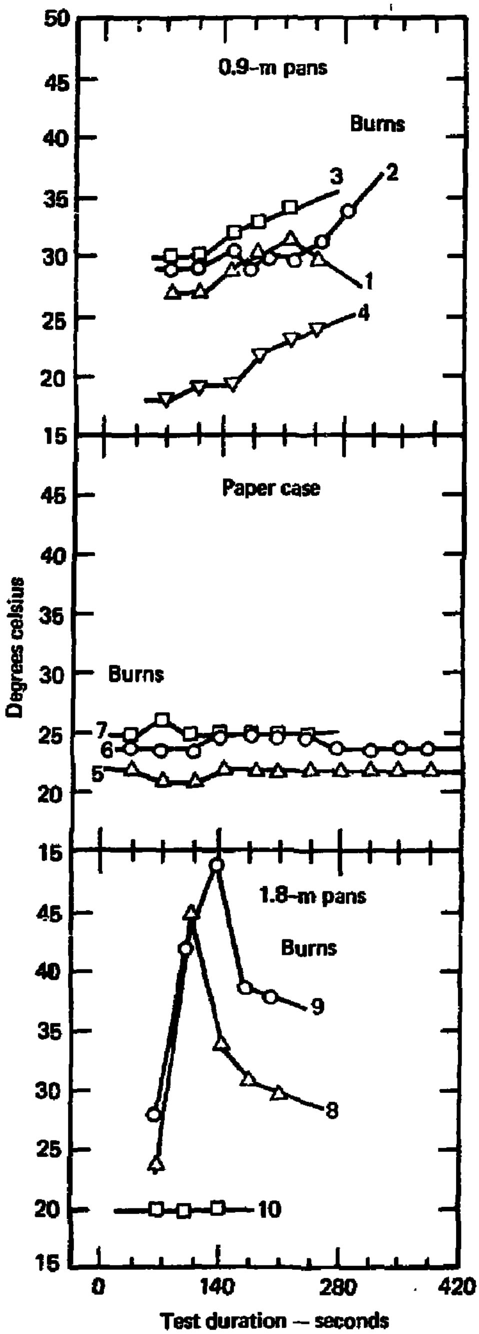

Fig. 9. Rate of temperature rise at ceiling (channel 0).

Radiant energy and total convective plus radiant energy measurements were made at station 1 (channel 12 and 13 respectively), while at stations 2 and 3, and in the south wall of the sheetrock shield, total heat flux measurements were made (channels 14, 15 and 11 respectively). Only peak values are reported in Table 1 because of the gross oscillation of the data. These oscillations resulted from turbulent smoke formation which attenuates thermal radiant heat transfer and from a wildly gyrating fire envelope. This wild fire behavior was caused by oxygen depletion within the sheetrocked fire pit. Both 0.9- and 1.8-m pan fires showed this behavior. The high-peak flux levels indicated at the south wall position (channel 11) were the result of direct fire contact with the sensing surface of the radiometer. The average flux level at this position was approximately 7 W/cm^2, which is an average value for flame contact heat transfer. These measurements indicate that the major mode of heat transfer, remote from the fire, is due to convection from the combustion gases.

Figure 10 is a composite of eight photographic plates showing the variable nature of the 1.8-m-pan fires. Plates 4 and 6 graphically illustrate the flame gyrations within the test enclosure. The flame tended to bathe the south wall of the enclosure, probably because of easier access of air from the north.

The fuel consumption rate values for the 0.9-m pan and the paper cage fires were experimentally determined. The rate values for the 0.9-m-pan fires varied from 60 to 100% of the theoretical rate, as indicated by heat release rate considerations. In each of these tests, the fuel load was identical. Figure 11 shows the reduction in normalized mass versus time for the 0.9-m-pan fires. There is considerable variation in these data which could be caused by temporary oxygen starvation within the test area.

Figure 12 shows the fuel consumption of the paper cage burns with time. In these tests the fuel load was changed for every test; thus the change in burning rate is expected and is in the correction direction.

The total weight of the 1.8-m-pan, water, and fuel load was too great for the capacity of the load cell. However, the extreme and random turbulence of the fire envelope suggests an oxygen-starved condition which could result in a reduced fuel consumption rate.

The photographic and video records show the following:

- The paper cage fires created essentially no visible smoke.
- The 0.9-m-pan fires caused partial obscuration of the east wall of the Astron pit in 2 to 3 min, and while smoke was apparent in the ceiling of the Bldg. 431 high bay, it was not of sufficient density to obscure or distort the view of the vent windows.

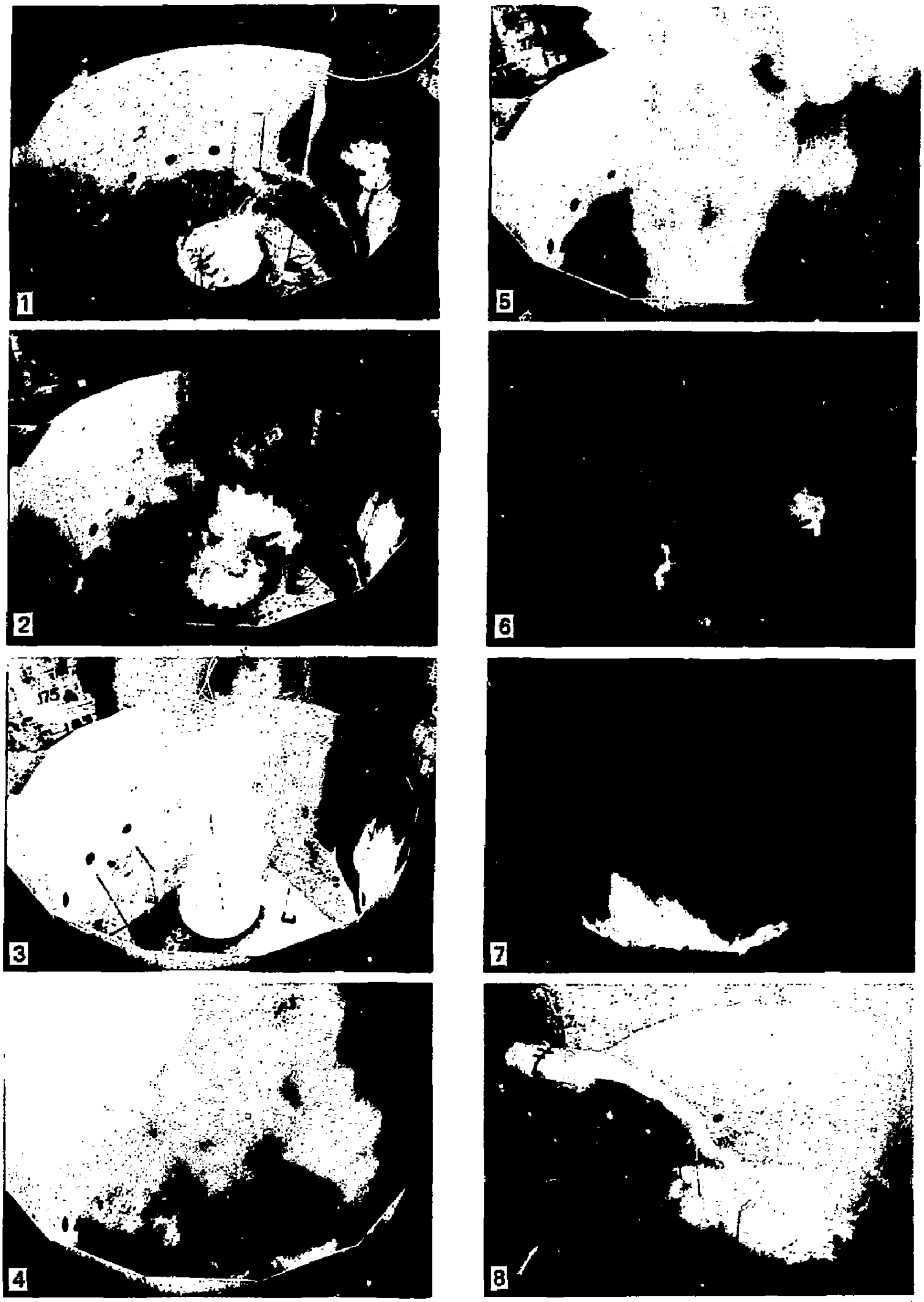

Fig. 10. Composite showing the variable nature of the 1.8-m-pan fires.

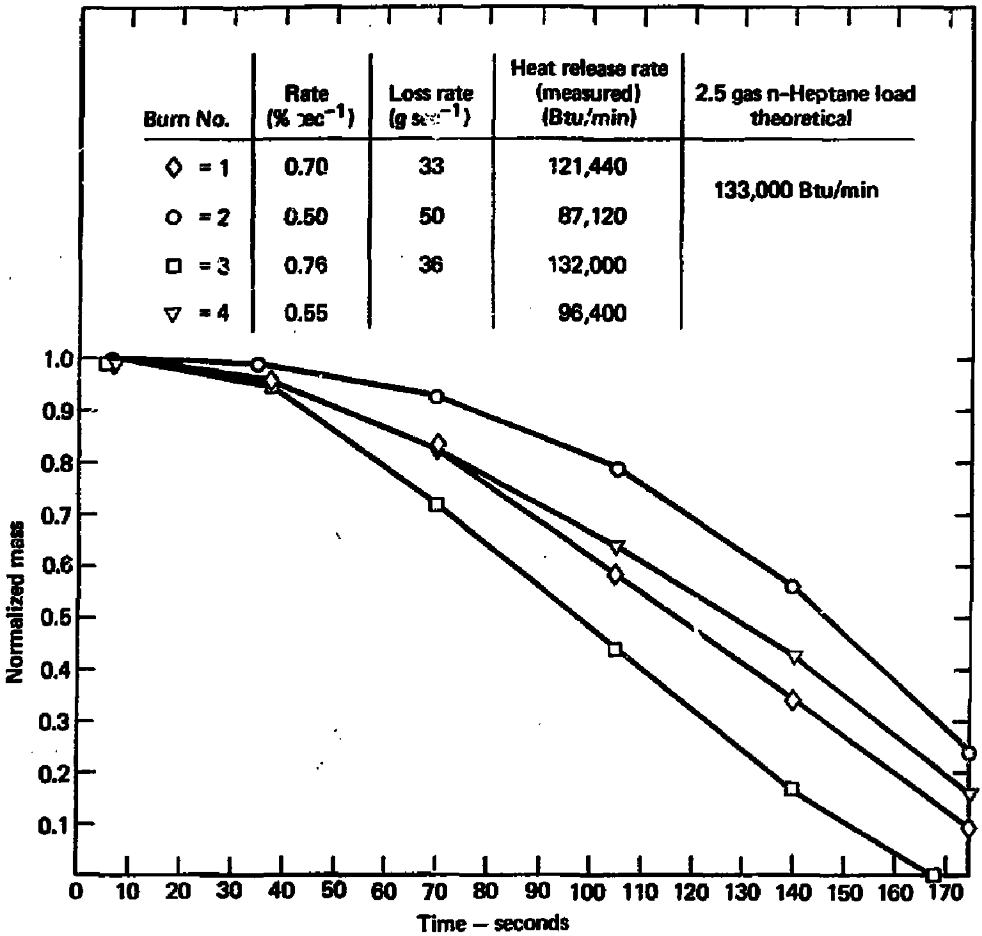

Fig. 11. Reduction of normalized mass vs time for 0.9-m-pan fires.

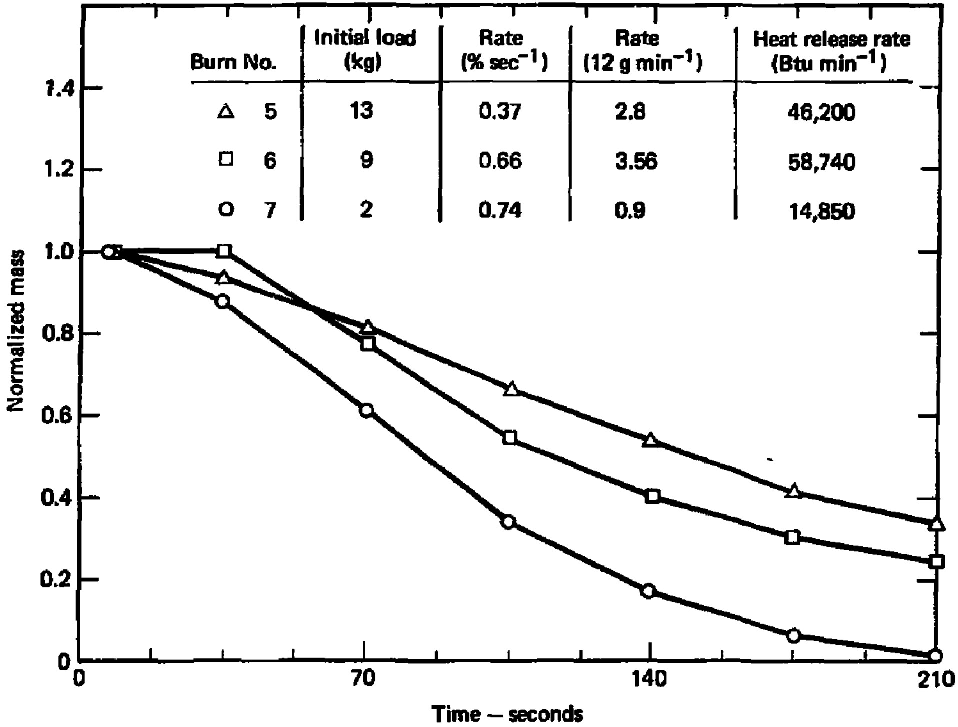
Burn No.
Initial load (kg)
Rate (% sec⁻¹)
Rate (12 g min⁻¹)
Heat release rate (Btu min⁻¹)
5
13
0.37
2.8
46,200
6
9
0.66
3.56
58,740
7
2
0.74
0.9
14,850
Normalized mass
1.4
1.2
1.0
0.8
0.6
0.4
0.2
0
0
70
140
210
Time — seconds

- The 1.8-m-pan fires produced smoke at very high rates; e.g., in the Astron bay, the east and north wall were obscured within 30 s of ignition. Smoke filled the entire Astron area to an uncomfortable concentration. In the high bay, for all three of the 1.8-m-pan burns the smoke billowed through both openings in the shielding roof, then drifted to the north side of the high bay. In 30 seconds the northeast windows were 50% obscured, and by 60 seconds they were almost 95% obscured. Light from the south windows was never attenuated more than 40 to 50%.

Table 2 lists the fire detector response times for the three sizes of test fires, in terms of their station location. At each station the detectors are listed in the order of increasing alarm times.*

Analysis of the data indicates the following trends, some of which should be intuitive:

- Larger fires (in terms of burning rate and smoke production) generally result in the alarm of more detectors.
- Detectors located directly over the fire are more likely to alarm than are detectors at other locations.
- Only beam-type and IR detectors will alarm at early times when located at mid-wall stations.
- Ionization detectors appeared to be the most sensitive and reliable of the detectors for sensing products of combustion.
- IR detectors were the fastest to alarm during the liquid fuel fire test.
- The beam-type detector appeared promising in terms of the remote sensing of fires, and also as a large area fire detection system. (Non-response to the fire plume of the 1.8-m pan fires was caused by the misalignment of the detector† and receiver module).

---

*Note that the goodness of a fire detector is not necessarily a function of the speed with which it responds to the specific fire signature it was designed to sense. A much more valid measure of quality is its reliability and uniformity of response. In fact, most good detectors have a built-in time lag to ensure reliable operation. However, a fast and reliable detector is very desirable.

†Because of our unfamiliarity with the operation of this detector, we were only able to operate in the "refractive index" mode. We have made subsequent tests with the device which showed successful response both in attenuation and refraction index modes.

- The cloud chamber detector successfully responded to the paper cage and 1.8-m pan fires when the alarm circuit was adjusted to the most sensitive setting.*
- The rate of temperature rise at station 1 was the same for both the three foot pan and the paper cage fires. However, the magnitude of temperature rise for the pan fires was approximately twice that of the paper cage (15°C and 7°C respectively). Apparently this difference is sufficient for tripping of the thermal detectors.

CONCLUSIONS

This test series was conducted to delineate several areas of concern as to the behavior of the combustion products plume from a large fire in Bldg. 431, and to generate some background information concerning the siting requirements and response of various types of fire and smoke detection systems. Questions were posed in the Introduction of this report, and we shall attempt to answer them, based on the data herein.

1. Q. How does the bouyant smoke plume underact with the normal ventilation patterns of the building?

   A. For the 0.9-m pan fires, the smoke appeared to diffuse uniformly into the high bay. However, during most of the 0.9-m series, most of the window vents were closed. During the 1.8-m-pan burns, the vents were open and smoke tended to concentrate on the north side. Workers in the side mezzanines noted the odor of smoke, but very minimal light scattering.

2. Q. Does Building 431 have a resident inversion layer?

   A. No, not in the weatner patterns of April 1977.

3. How long does it take:

   Q. For smoke to reach the ceiling?

   A. Approximately 15 seconds for 1.8-m-pan fires.

   Q. To fill the ceiling space:

   A. Approximately 60 seconds for 1.8-m-pan fires.

---

*At the most sensitive setting, there appears to be no discrimination between the channels. Perhaps the optical cell does not clear as well in this operational mode. Note also that the time delay between smoke reaching the intake orifice of the detector and the end of the sensing tube was of the order of 60 seconds.

Q. To fill the shielded area:

A. About 60 seconds for 1.8-m-pan fires.

Q. To activate strategically placed detector arrays?

A. See Table 2.

4. Q. What is the temperature rise in the high bay ceiling? In the shielded area? At the detector arrays for various fire sizes and types?

A. See Table 1.

5. Q. Will the existing ceiling vents remove significant quantities of smoke and heat?

A. If the fire is of long duration, or large, it does not appear that the existing ceiling vents could remove sufficient quantities of smoke to keep the building habitable.

6. Q. Under venting conditions, will the ceiling air temperature rise be of sufficient rate to fuse the ceiling sprinklers?

A. Under conditions of high ambient temperature, it appears that large fires could cause sprinklers to fuse.

7. Q. What type(s) of detectors respond most reliably to the types and sizes of fires that have some probability of occurrence in the MFTF area?

A. If we were to rate fire potential in a descending order of probability, we would count fires in electronic components and electrical insulation fires from electrical overloads as high on the list. At the other end of the probability spectrum would be fires in dielectric fluids. In between would be fire potentials which could range from trash fires to fires occurring in materials brought into the area of concern during periods of construction. The fires starts of high probability would be small, smouldering types, while those of low probability would include large, energetic disasterous-type fires.

The included tests indicated that ion- and IR-type detectors sensed all fires. Thus, some combination of these two detector types appears most reliable at the current level of technology.

8. Q. What types of fire suppressant strategies provide a feasible solution to the major potential fuel source projects for MFTF?

A. No single extinguisher is a panacea for the potential fuel mix available in the MFTF enclosure. Areas which have unusual and similar fuel loads need to be concentrated and specific extinguishing strategies applied to them; e.g., AFFF over liquid fuel reservoirs, Hi-X over large electronic components, inert gases for sensitive electronic controls, etc.

9. Q. What logic can be used to identify sites for location of detection and suppression arrays?

A. Many detectors are sensitive to ionizing radiation and consequently, cannot be used in areas of high radiation background. However, the instruments are compromised only during periods when the ionizing radiation is present. This condition should exist only when the MFTF is in operation, at which time there should be sufficient personnel in attendance to observe any unwanted ignitions. The detectors can be activated during periods of experimental modification or inactivity. IR detectors should be placed such that the supervised item is included in its field of view, and ion detectors should be placed in areas where the potential smoke will collect or stagnate (i.e., relatively close to the ceiling). Ion detectors in exit ducts of the ventilation system are advisable.

10. Q. Which components of smoke are most readily detectable in large volume enclosures?

A. Both electromagnetic radiation from flames and combustion or pyrolysis products are locally detectable. For remote detection, smoke attenuation and the refractive index change of the combustion gas column appear to be detectable by beam-type detectors.

VRS/bjt/lr

Printed in the United States of America
Available from
National Technical Information Service
U.S. Department of Commerce
5285 Port Royal Road
Springfield, VA 22161
Price: Printed Copy $ $4.50 ; Microfiche $3.00

Page Range	Domestic Price	Page Range	Domestic Price
001-025	$ 4.00	326-350	$12.00
026-050	4.50	351-375	12.50
051-075	5.25	376-400	13.00
076-100	6.00	401-425	13.25
101-125	6.50	426-450	14.00
126-150	7.25	451-475	14.50
151-175	8.00	476-500	15.00
176-200	9.00	501-525	15.25
201-225	9.25	526-550	15.50
226-250	9.50	551-575	16.25
251-275	10.75	576-600	16.50
276-300	11.00	601-up	—[1]
301-325	11.75		

[1] Add $2.50 for each additional 100 page increment from 601 pages up.